



Measurement of Optical Constants of TiN and TiN/Ti/TiN Multilayer Films for Microwave Kinetic Inductance Photon-Number-Resolving Detectors

M. Dai¹ · W. Guo² · X. Liu³ · M. Zhang³ · Y. Wang³ · L. F. Wei¹ · G. C. Hilton² · J. Hubmayr² · J. Ullom² · J. Gao² · M. R. Vissers²

Received: 9 November 2017 / Accepted: 14 November 2018 / Published online: 18 December 2018
© Springer Science+Business Media, LLC, part of Springer Nature 2018

Abstract

We deposit thin titanium nitride (TiN) and TiN/Ti/TiN multilayer films on sapphire substrates and measure the reflectance and transmittance in the wavelength range from 400 to 2000 nm using a spectrophotometer. The optical constants (complex refractive indices), including the refractive index n and the extinction coefficient k , have been derived. With the extracted refractive indices, we propose an optical stack structure using low-loss amorphous Si (a-Si) anti-reflective coating and a backside aluminum (Al) reflecting mirror, which can in theory achieve 100% photon absorption at 1550 nm. The proposed optical design shows great promise in enhancing the optical efficiency of TiN-based microwave kinetic inductance photon-number-resolving detectors.

Keywords Optical constants · Refractive index · TiN · Microwave kinetic inductance detectors

1 Introduction

Photon-number-resolving (PNR) detectors are able to directly measure the photon number and energy in a pulse of incident light. In particular, the PNR detectors at visible and near-infrared wavelengths have important applications in many fields such

✉ L. F. Wei
lfwei@swjtu.edu.cn

Y. Wang
yiwenwang.nju@gmail.com

¹ Information Quantum Technology Laboratory, School of Information Science and Technology, Southwest Jiaotong University, Chengdu 610031, China

² National Institute of Standards and Technology, Boulder, CO 80305, USA

³ Quantum Optoelectronics Laboratory, School of Physical Science and Technology, Southwest Jiaotong University, Chengdu 610031, China

as quantum secure communications [1], linear optics quantum computing [2], quantum optics experiments [3] and optical quantum metrology [4]. To meet the requirements of these applications, an ideal PNR detector should have both high energy resolution and high system detection efficiency. By minimizing the fiber-to-detector coupling losses and using optical stack structures that enhance the photon absorption by the absorber material, transition edge sensors (TESs) have demonstrated high energy resolution and near unity system detection efficiency at near-infrared wavelengths [5–11].

Another type of superconducting detector with intrinsic photon-number-resolving and energy-resolving capability is the microwave kinetic inductance detector (MKID) [12]. As compared to TESs, MKIDs are easy to fabricate and multiplex into large arrays. Single-photon counting at telecommunication wavelengths (near-infrared) with titanium nitride (TiN) MKIDs was first demonstrated in reference [13]. Recently, by optimizing the MKID design, we have achieved an energy resolution of 0.22 eV and resolved up to 7 photons per optical pulse at 1550 nm using MKIDs made from TiN/Ti/TiN trilayer films [14]. Although the energy resolution of these detectors is already impressive, little effort has been made to improve their optical efficiency.

The major sources that limit the optical efficiency of MKIDs include fiber-to-detector coupling efficiency, photon loss due to reflection from and transmission through the thin TiN layer. As the first step to improve the optical efficiency of photon-number-resolving TiN-MKIDs, in this paper, we show measurements of the optical constants (complex refractive indices) for thin TiN and TiN/Ti/TiN multilayer films. We then propose an optical stack structure that can in theory achieve 100% photon absorption at 1550 nm for TiN-based MKIDs.

2 Principle

In this section, we briefly introduce the optical transfer matrix theory which is commonly used to obtain the reflectance R and transmittance T [15] for a multilayer optical structure.

Consider a beam of light from the air is normally incident onto an optical stack consisting of K layers and exit into the air. Assume the refractive index of air is 1 and each layer has thickness of d_j and complex refractive index of $\tilde{n}_j = n_j - ik_j$ (here n_j and k_j are wavelength λ -dependent refractive index and extinction coefficient for the j -th layer, $j = 1, \dots, K$), the magnitude of the incident electromagnetic wave $[E_0 \ B_0]^T$ and the transmitted wave $[E_{K+1} \ B_{K+1}]^T$ are related by the products of the transfer matrices as

$$\begin{bmatrix} \mathbf{E}_0 \\ \mathbf{H}_0 \end{bmatrix} = \left\{ \prod_{j=1}^K \begin{bmatrix} \cos(k\tilde{n}_j d_j) & i \cdot \sin(k\tilde{n}_j d_j)/\tilde{n}_j \\ i \cdot \tilde{n}_j \sin(k\tilde{n}_j d_j) & \cos(k\tilde{n}_j d_j) \end{bmatrix} \right\} \begin{bmatrix} \mathbf{E}_{K+1} \\ \mathbf{H}_{K+1} \end{bmatrix} \quad (1)$$

$$\begin{bmatrix} B \\ C \end{bmatrix} = \left\{ \prod_{j=1}^K \begin{bmatrix} \cos(k\tilde{n}_j d_j) & i \cdot \sin(k\tilde{n}_j d_j)/\tilde{n}_j \\ i \cdot \tilde{n}_j \sin(k\tilde{n}_j d_j) & \cos(k\tilde{n}_j d_j) \end{bmatrix} \right\} \begin{bmatrix} 1 \\ 1 \end{bmatrix} \quad (2)$$

where k is wave factor. $[B \ C]^T$ is called the characteristic matrix of dielectric film. It follows from Eqs. (1, 2) that the reflectance and transmittance of the whole optical stack are given by

$$R(\lambda, n_j, k_j, d_j) = \left| \frac{B - C}{B + C} \right|^2, \quad (3)$$

$$T(\lambda, n_j, k_j, d_j) = \left| \frac{2}{B + C} \right|^2, \quad (4)$$

Equations (3, 4) allow us to solve for the n and k values of a layer in the optical stack from the combined measurements of the reflectance R and transmittance T , if we know the complex refractive indices for all the other layers and the thickness of all the layers. In Sect. 3, we use this method to extract the complex refractive indices for thin TiN and TiN/Ti/TiN multilayer films deposited on thick sapphire substrates. On the other hand, when the complex refractive indices $n_j - ik_j$ and thickness d_j of each layer are given, Eqs. (3, 4) also allow us to directly calculate the wavelength dependent $R(\lambda)$ and $T(\lambda)$ of the multilayer stack, which is used in Sect. 4 to design the optimized optical structure that can maximize the photon absorption at 1550 nm.

3 Measurements of Optical Constants

We deposited thin stoichiometric TiN and TiN/Ti/TiN multilayer films on 500- μm -thick double-side polished sapphire substrates. The multilayer film comprises a stack of 7 layers with TiN at the top and bottom interface and alternating layers of Ti and TiN in the middle. The detailed deposition conditions and processes can be found in reference [16, 17]. To precisely determine the optical constants of these thin films, one should properly choose the film thickness. On the one hand, if the film is too thin, the uncertainty in the film thickness will result in large errors in the derived n and k values. On the other hand, if the film is too thick, the transmitted light will be too weak to be measured accurately due to instrument noise and background stray light. We have chosen a target thickness of 60 nm for both films. The actual thicknesses were carefully measured by a profilometer which reports 63 nm for the stoichiometric TiN film and 43 nm for the TiN/Ti/TiN multilayer.

The reflectance R and transmittance T in the wavelength range from 400 to 2000 nm were measured (not simultaneously) at room temperature using a commercial spectrophotometer (PerkinElmer's LAMBDA 1050). The reflection measurement is performed with a standard UV/NIS/NIR Universal reflectance accessory, and the angle between the sample and the incident beam is set to 8° . The transmission is measured by a standard 3D wideband detector module, and the incident beam is normal to the sample. The reflection and transmission curves are almost coincident ($< 0.1\%$ difference) for incident angles below 10° . The experimental results are shown in Fig. 1a, b, respectively. From the R and T data, it is straightforward to obtain the absorption

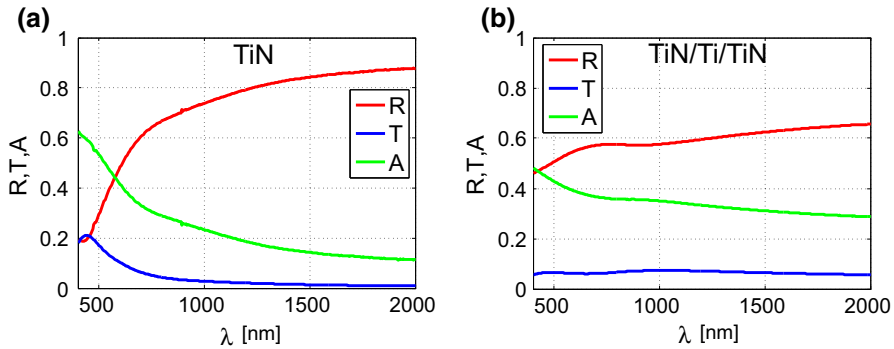


Fig. 1 Measurements of the reflectance R and transmittance T for: **a** 63 nm stoichiometric TiN film on a 500- μm -thick sapphire substrate. **b** 43 nm TiN/Ti/TiN multilayer film on a 500- μm -thick sapphire substrate (Color figure online)

as $A = 1 - R - T$, which is of practical interest since it directly affects the optical efficiency.

We also measured the R and T data for a 500- μm -thick double-side polished bare sapphire wafer, which can be easily analyzed with the transfer matrix theory introduced in Sect. 2 to give the complex refractive index of sapphire ($n_2 = 1.75$ and $k_2 = 0$), which is approximately wavelength independent. We find the measured optical constants of sapphire match well with the tabulated values [18]. For the two-layer stack of TiN film on sapphire substrate, we have the measured thickness of the TiN layer ($d_1 = 63$ nm for stoichiometric TiN and 43 nm for TiN/Ti/TiN multilayer), the vendor specified wafer thickness ($d_2 = 500$ μm) and the derived complex refractive index ($n_2 = 1.75$ and $k_2 = 0$) of the sapphire substrate. Then, Eq. (3, 4) reduce to two nonlinear equations with two unknown variables (n_1 and k_1 of the TiN layer),

$$\begin{cases} R(n_1, k_1; \lambda, n_2, k_2, d_2) = R_{\text{mea}} \\ T(n_1, k_1; \lambda, n_2, k_2, d_2) = T_{\text{mea}} \end{cases}, \quad (5)$$

where R_{mea} and T_{mea} are the measured reflectance and transmittance data. The above equations can be solved numerically [15] at a specific wavelength λ . Note that we take the thick-substrate approximation [19] that assumes reflections off the back surface add incoherently so that we can get smooth n and k vs. wavelength curve.

Figure 2a, b plots the derived refractive index n and extinction coefficient k as a function of wavelength. For stoichiometric TiN film, one can see a low refractive index in the visible wavelength and even $n < 1$ at the wavelength range from 570 to 712 nm, which is similar to previous optical measurements on TiN films [20,21]. It is worth mentioning that n is the refractive index indicating the phase velocity and is frequency dependent. In some cases, one can have phase velocity greater than the speed of light in vacuum (without violating the relativity); thus, n less than 1 can occur. The n for TiN/Ti/TiN multilayer is higher and increases monotonically with wavelength, which resembles the properties of pure Ti film. k ranging from 2 to 6 is also a signature of pure Ti film [18]. Strictly speaking, the optical constants n and k should also be

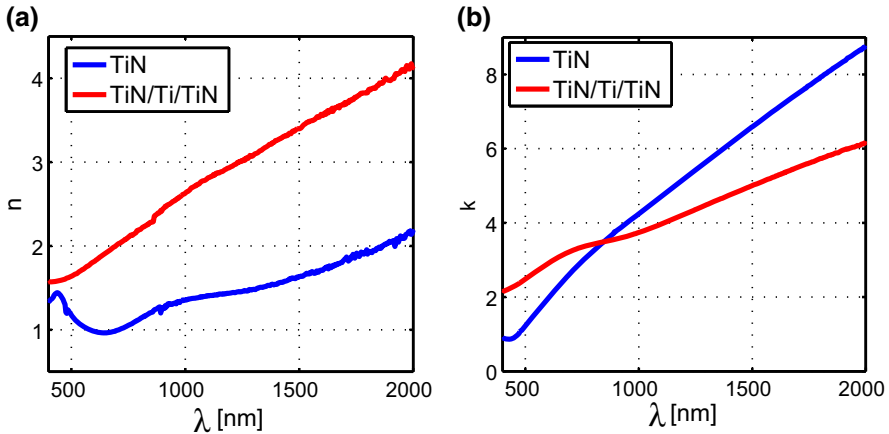


Fig. 2 The derived optical constants (n and k) versus wavelength. The blue and red curves represent stoichiometric TiN and TiN/Ti/TiN multilayer films, respectively (Color figure online)

dependent on the film thicknesses, which needs to be experimentally investigated in the future work.

4 Optical Designs for Enhancement of Photon Absorption

In this section, we use the n and k values derived in the previous section to design optimal stack structures that can enhance the photon absorption efficiency at a particular wavelength. In the following, we mainly discuss the designs for TiN/Ti/TiN multilayers at 1550 nm, because photon-number-resolving MKIDs based on TiN/Ti/TiN multilayer films have already demonstrated high energy resolution and good multiphoton discrimination capability at 1550 nm [14], and also because the TiN/Ti/TiN multilayer has superior uniformity (as compared to substoichiometric TiN films) which is critical for scaling into large MKID arrays.

We present two optical designs for enhancing photon absorption in TiN/Ti/TiN multilayer films. The first relative simple structure includes a single amorphous Si (a-Si) anti-reflective (AR) coating layer deposited on top of a 43-nm-thick TiN/Ti/TiN multilayer film. We use the thickness (43 nm) of the measured film for this design, so we can safely use the measured n and k for simulation. We choose a-Si because it has shown reduced two-level systems (TLSs) and low microwave loss comparing to other dielectric materials, such as SiO_2 and Si_3N_4 [22,23]. We choose a relative thick (43 nm) TiN/Ti/TiN multilayer film to enhance the absorption in the film and prevent light from penetrating the film. Using the extracted values of n and k , we calculate expected performance of this structure in terms of reflectance, transmittance and absorption at 1550 nm wavelength as a function of the thickness of a-Si AR coating. As shown in Fig. 3a, the absorption varies periodically with the thickness of Si layer and a maximum absorption of 68% is first reached at a coating thickness of 113 nm, which suggests an optimal design illustrated by the cartoon in Fig. 3a. Figure 3b shows

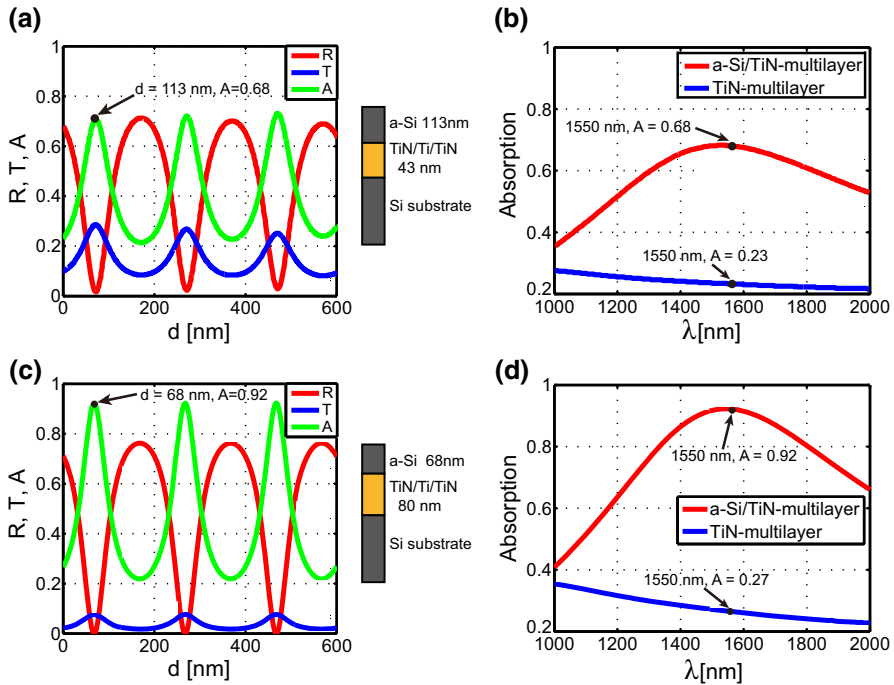


Fig. 3 **a** The simulated reflectance R , transmittance T and absorption A at 1550 nm of AR-coated TiN/Ti/TiN multilayer (43 nm thick), showing a periodical change as a function of the thickness of the a-Si AR layer. With a 113-nm-thick a-Si AR layer, the absorption can reach a maximum of 68%. The stack structure as well as the thicknesses of each layer is illustrated by the small cartoon to the right. **b** Comparison of the absorption A by 43-nm-thick TiN/Ti/TiN multilayer with (red curve) and without AR coating (blue curve) in the near-infrared wavelength, which clearly show the AR coating can significantly improve the absorption. **c** The simulation results for 80-nm-thick TiN/Ti/TiN multilayer with a-Si AR coating. **d** Comparison of the absorption A by 80-nm-thick TiN/Ti/TiN multilayer with (red curve) and without AR coating (blue curve) (Color figure online)

the simulated absorption of this optimal stack (red curve) between 1000 and 2000 nm, which is compared to the TiN/Ti/TiN multilayer film alone without AR coating (blue curve). It is clear that the AR coating design has significantly enhanced the absorption, from less than 30 to 68% around 1550 nm. If we assume that the optical constants n and k of the TiN/Ti/TiN multilayer do not significantly change with its thickness, we also show the design for 80-nm-thick TiN/Ti/TiN multilayer film in Fig. 3c, d. With one layer of 68-nm-thick a-Si AR coating, the maximum absorption is improved from 27 to 92% for the design with 80-nm-thick TiN film, indicating the absorption can be improved by increasing the absorber thickness.

While the single-layer a-Si AR coating solution is attractive and relative easy to implement (and we plan to test it in the future), the theoretical maximum absorption is still less than unity, so we further propose another optical stack design that can achieve 100% absorption at 1550 nm. In this design, a 43-nm-thick TiN/Ti/TiN trilayer film is sandwiched between two a-Si layers of different thicknesses and a thick aluminum (Al) layer is buried under the sandwich. We use an Al layer as a bottom mirror to

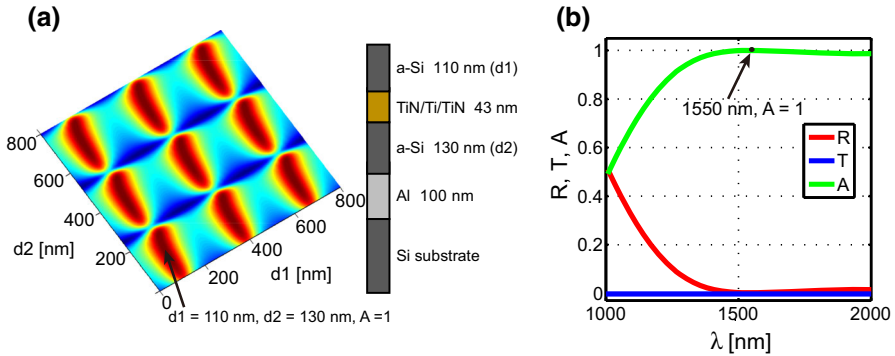


Fig. 4 **a** The simulated absorption of a 43-nm-thick TiN/Ti/TiN trilayer versus thicknesses of the top (d_1) and bottom (d_2) a-Si layers in the proposed optical cavity structure. The stack structure as well as the optimal thickness of each layer is illustrated by the small cartoon to the right. **b** The simulated wavelength-dependent reflectance R , transmittance T and absorption A of TiN/Ti/TiN multilayer film embedded in the optimized optical cavity structure (Color figure online)

create an optical cavity and embed the thin TiN/Ti/TiN trilayer film in the cavity to enhance the absorption. An important reason for choosing Al (instead of Au as used in optical TES) as the mirror material is that Al is superconducting which is expected not to introduce metal losses and degrade the quality factor of the MKIDs.

Figure 4a shows the simulated absorption at 1550 nm in the two-dimensional parameter space of the two a-Si layer thicknesses (d_1 and d_2). The absorption varies periodically with d_1 and d_2 , and a maximum absorption of unity is first reached at $d_1 = 110$ nm and $d_2 = 130$ nm. The stack structure with optimal layer thicknesses is illustrated by the cartoon to the right of Fig. 4a. In Fig. 4b, we plot the wavelength-dependent absorption of this optimal stack structure, which shows that 100% absorption and 0% reflectance have been achieved at the wavelength of 1550 nm. In principle, 100% absorption for this stack structure can be achieved no matter how thin the TiN multilayer film is, as long as we optimize the two a-Si layer thicknesses. A thinner TiN film is preferred because we found that smaller absorber volume corresponds to larger responsivity and better energy resolution in our previous photon-counting experiment [14].

Note that in this work we use room-temperature measurements to design the optical stack structure working at cryogenic temperature. (The operation temperature of MKIDs is usually below 100 mK.) However, the question of how optical constants vary when thin films are cooled from room temperature to cryogenic temperature is a valid question in both theory and experiments. In theory, it is well known that far above the superconducting energy gap 2Δ , a superconductor behaves like a normal metal in the optical response [24]. For photons with energy $\hbar\omega \gg 2\Delta$, the states originally within $\hbar\omega$ of the occupied states below the Fermi level are all available for excitation and the gap effects are negligible. We can also directly look at the optical constants. If we assume the relative magnetic permeability ~ 1 (a reasonable approximation for most solids), the complex index of refraction \tilde{n} is equal to the square root of the dielectric function, which is then related to the complex conductivity. The

temperature and frequency dependence of the complex conductivity can be derived from the well-established Mattis–Bardeen theory, showing that at high frequency limit ($\gg 2\Delta$), the complex conductivity has little temperature dependence [24]. For the stoichiometric TiN and TiN/Ti/TiN multilayer films used in our experiments, their T_c is about 4 K and 1.4 K, respectively. According to the BCS theory, $2\Delta/k_B T_c = 3.5$, T_c of 4 K corresponds to energy gap $2\Delta \approx 2.9 \times 10^{11}$ Hz, which is far below the near-infrared frequency range. Therefore, the optical properties of TiN films at visible and near-infrared wavelengths (400–2000 nm in this work) are expected to have little change from room temperature to ultra-low temperature. In experiments, people have verified that superconducting films and normal-state films have little difference in optical properties. For example, the NIST researchers measured the reflectance of the tungsten film (optical absorber for TES) at 3.2 K using a swept wavelength interferometer and found that the low-temperature reflectance at the target wavelength matched the room-temperature reflectance [7]. Besides, the reflectance of thin TiN film has also been measured for a broad spectral range from the far infrared (IR) up to the ultraviolet (UV), and no temperature dependence is observed between 2 and 300 K measurements [25]. Therefore, we can conclude that optical constants do not change significantly at cryogenic temperatures, so one can use measurements done at room temperature to predict performance at cryogenic temperatures. In practice, with the optical constants n and k of the TiN films obtained from the room-temperature measurement, we can theoretically determine the optimum thickness of the AR coating for the maximum absorption. Then, we can prepare multiple samples with same TiN film but coated with a-Si with various thicknesses around the theoretical optimum value, and search the best coating thickness through measurements at cryogenic temperature. This in turn will provide information to improve our next design.

5 Conclusion

We have successfully determined the optical constants (refractive index n and extinction coefficient k) of superconducting stoichiometric TiN and TiN/Ti/TiN multilayer thin films, from combined measurements of reflectance and transmittance at the wavelength ranging from 400 to 2000 nm. By utilizing the extracted n and k values, two optical stack designs have been presented and discussed, which may significantly improve photon absorption into TiN/Ti/TiN multilayer films. In particular, by embedding the TiN/Ti/TiN film in an optical cavity structure one may in theory achieve unity absorption at 1550 nm. The proposed designs show great promise in achieving high system detection efficiency in near-infrared photon-number-resolving TiN MKIDs.

Acknowledgements The TiN films were deposited in the NIST-Boulder micro-fabrication facility. We thank Dr. Adriana. E. Lita for useful discussions. This work was supported in part by the National Natural Science Foundation of China (Grant Nos. 61871333, 61301031, U1330201).

References

1. P.A. Hiskett, D. Rosenberg, C.G. Peterson, R.J. Hughes, S. Nam, A. Lita, A. Miller, J. Nordholt, *New J. Phys.* **8**(9), 193 (2006)
2. E. Knill, R. Laflamme, G.J. Milburn, *Nature* **409**(6816), 46–52 (2001)
3. M. Giustina, A. Mech, S. Ramelow, B. Wittmann, J. Kofler, J. Beyer, A. Lita, B. Calkins, T. Gerrits, S.W. Nam et al., *Nature* **497**(7448), 227–230 (2013)
4. J.C. Zwinkels, E. Ikonen, N.P. Fox, G. Ulm, M.L. Rastello, *Metrologia* **47**(5), R15 (2010)
5. A.J. Miller, S.W. Nam, J.M. Martinis, A.V. Sergienko, *Appl. Phys. Lett.* **83**(4), 791–793 (2003)
6. A.E. Lita, A.J. Miller, S.W. Nam, *Opt. Express* **16**(5), 3032–3040 (2008)
7. A.E. Lita, B. Calkins, L.A. Pellouchoud, A.J. Miller, S. Nam, *Proc. SPIE* **7681**, 76810D (2010)
8. B. Calkins, P.L. Mennea, A.E. Lita, B.J. Metcalf, W.S. Kolthammer, A. Lamas-Linares, J.B. Spring, P.C. Humphreys, R.P. Mirin, J.C. Gates et al., *Opt. Express* **21**(19), 22657–22670 (2013)
9. L. Lolli, E. Taralli, M. Rajteri, *J. Low Temp. Phys.* **167**(5–6), 803–808 (2012)
10. G. Brida, L. Ciavarella, I.P. Degiovanni, M. Genovese, L. Lolli, M.G. Mingolla, F. Piacentini, M. Rajteri, E. Taralli, M.G. Paris, *New J. Phys.* **14**(8), 085001 (2012)
11. L. Lolli, E. Taralli, C. Portesi, E. Monticone, M. Rajteri, *Appl. Phys. Lett.* **103**(4), 041107 (2013)
12. P.K. Day, H.G. LeDuc, B.A. Mazin, A. Vayonakis, J. Zmuidzinis, *Nature* **425**(6960), 817–821 (2003)
13. J. Gao, M.R. Vissers, M.O. Sandberg, F.C.S. da Silva, S.W. Nam, D.P. Pappas, D.S. Wisbey, E.C. Langman, S.R. Meeker, B.A. Mazin, H.G. Leduc, J. Zmuidzinis, K.D. Irwin, *Appl. Phys. Lett.* **101**(14), 142602 (2012). <https://doi.org/10.1063/1.4756916>
14. W. Guo, X. Liu, Y. Wang, Q. Wei, L.F. Wei, J. Hubmayr, J. Fowler, J. Ullom, L. Vale, M.R. Vissers, J. Gao, *Appl. Phys. Lett.* **110**(21), 212601 (2017). <https://doi.org/10.1063/1.4984134>
15. J.E. Nestell, R.W. Christy, *Appl. Opt.* **11**(3), 643–651 (1972). <https://doi.org/10.1364/AO.11.000643>
16. M.R. Vissers, J. Gao, D.S. Wisbey, D.A. Hite, C.C. Tsuei, A.D. Corcoles, M. Steffen, D.P. Pappas, *Appl. Phys. Lett.* **97**(23), 232509 (2010). <https://doi.org/10.1063/1.3517252>
17. M.R. Vissers, J. Gao, M. Sandberg, S.M. Duff, D.S. Wisbey, K.D. Irwin, D.P. Pappas, *Appl. Phys. Lett.* **102**(23), 232603 (2013). <https://doi.org/10.1063/1.4804286>
18. <https://www.filmetrics.com/refractive-index-database>
19. D. Rosenberg, S. Nam, A. Miller, A. Salminen, E. Grossman, R. Schwall, J. Martinis, Nuclear instruments and methods in physics research section A: accelerators. *Spectrom. Detect. Assoc. Equip.* **520**(1), 537–540 (2004)
20. E. Valkonen, C.-G. Ribbing, J.-E. Sundgren, *Appl. Opt.* **25**(20), 3624–3630 (1986). <https://doi.org/10.1364/AO.25.003624>
21. B. Karlsson, J.-E. Sundgren, B.-O. Johansson, *Thin Solid Films* **87**(2), 181–187 (1982)
22. D. Smith, E. Shiles, M. Inokuti, E. Palik, *Handb. Opt. Constants Solids I*, 369–406 (1985)
23. J.M. Martinis, K.B. Cooper, R. McDermott, M. Steffen, M. Ansmann, K. Osborn, K. Cicak, S. Oh, D.P. Pappas, R.W. Simmonds et al., *Phys. Rev. Lett.* **95**(21), 210503 (2005)
24. M. Dressel, *Adv. Condens. Matter Phys.* **2013**, 104379 (2013)
25. F. Pfuner, L. Degiorgi, T. Baturina, V. Vinokur, M. Baklanov, *New J. Phys.* **11**(11), 113017 (2009)